Received: 15 October 2021 | Revised: 8 December 2021 | Accepted: 3 January 2022

DOI: 10.1002/aic.17588

PARTICLE TECHNOLOGY AND FLUIDIZATION

AIChE JOURNAL

Performance of limestone-based sorbent for sorption-enhanced gasification in dual interconnected fluidized bed reactors

Antonio Coppola[1] | Aida Sattari[2,3] | Fabio Montagnaro[2] | Fabrizio Scala[1,3] | Piero Salatino[1,3]

[1]Istituto di Scienze e Tecnologie per l'Energia e la Mobilità Sostenibili, Consiglio Nazionale delle Ricerche, Naples, Italy

[2]Dipartimento di Scienze Chimiche, Università degli Studi di Napoli Federico II, Complesso Universitario di Monte Sant'Angelo, Naples, Italy

[3]Dipartimento di Ingegneria Chimica, dei Materiali e della Produzione Industriale, Università degli Studi di Napoli Federico II, Naples, Italy

Correspondence
Fabio Montagnaro, Dipartimento di Scienze Chimiche, Università degli Studi di Napoli Federico II, Complesso Universitario di Monte Sant'Angelo, 80126 Naples, Italy.
Email: fabio.montagnaro@unina.it

Abstract

A possibility to carry out sorption-enhanced gasification (SEG) is represented by its integration with the calcium looping concept in dual interconnected fluidized beds (DIFB). This article is focused on the sorbent CO_2 uptake performance and attrition/fragmentation tendency when operating conditions simulating those of a DIFB-SEG process are adopted. Experiments were carried out on a commercial Italian limestone in a laboratory-scale DIFB reactor. Carbonation was carried out in a range of test conditions, including variable temperature (600–700°C) and absence/presence of steam (10% by volume); CO_2 concentration was set at 10% by volume. The characterization is extended by investigating the behavior of preprocessed DIFB-SEG samples on impact fragmentation tests, conducted in an *ex situ* apparatus. Tests were carried out for impact velocities in the range 17–45 m/s. Results were discussed considering both the impact velocity value and the operating conditions under which the sample was preprocessed in the fluidized bed.

KEYWORDS
attrition, CO_2 capture, fluidized beds, gasification, impact fragmentation, limestone sorbent

1 | OVERVIEW

Sorption-enhanced gasification (SEG) is a relatively novel and promising concept that can be based, for example, on the use of inexpensive and widely available Ca-based sorbent (like limestone) to remove CO_2 from the syngas *in situ* during gasification (e.g., steam gasification) of a solid fuel, either renewable, waste-derived or fossil. Continuous *in situ* CO_2 sorption pushes the equilibrium of the water-gas shift reaction ($CO + H_2O = CO_2 + H_2$) toward the products, resulting in H_2-enriched syngas (up to 80% by vol.).[1] Moreover, the presence of Ca in the gasification environment can exert a catalytic effect[2,3] in the reforming of fuel-derived tars toward less harmful products (e.g., CO, CO_2) and H_2. The SEG process can benefit to a large extent from borrowing the extensive understanding and characterization of the calcium looping (CaL) process, a post-combustion technique aimed at removing CO_2 from flue gas. CaL is most typically carried out in a dual interconnected fluidized beds (DIFB) reactor scheme with a Ca-based sorbent being cycled between the carbonator, where it captures CO_2 from flue gas, and the calciner, where the sorbent releases concentrated CO_2 and is regenerated for another cycle.[4–11]

A scheme of the process is illustrated in Figure 1. DIFB reactors stem out as a natural choice for carrying out SEG[12,13] according to the following main reasons: (i) heterogeneous reactions, involving both

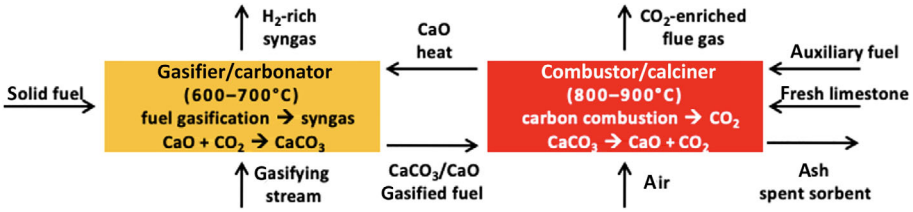

FIGURE 1 Outline of sorption-enhanced gasification in dual interconnected fluidized beds reactor

the sorbent and the fuel, are conveniently carried out in fluidized beds, due to the very efficient mixing, heat/mass transfer, and temperature control; (ii) circulation of granular solids from one reaction environment to the other is easily accomplished when the particles are in fluidized state. Solid fuel is fed to the gasifier-carbonator together with the gasifying stream (steam/oxygen). Gasification takes place at circa 600–700°C yielding a primary syngas with C/H ratio that depends on the operating conditions. At the same time, the reactor is fed with a stream of CaO: CO_2 capture from the primary syngas occurs via sorbent carbonation ($CaO + CO_2 \rightarrow CaCO_3$), active in this temperature range, yielding: (i) a secondary syngas rich in H_2 (and depleted in CO_2); (ii) a solid stream of carbonated sorbent (plus unconverted CaO) and gasified solid char, with residual carbon content. The latter stream is sent to the combustor-calciner, operated in the range 800–900°C, where it is contacted with air and, if needed, additional fuel. In this reactor, the sorbent is regenerated due to calcination ($CaCO_3 \rightarrow CaO + CO_2$), to produce a CaO stream ready for further cycling. Combustion of residual carbon and use of auxiliary fuel in the calciner must be tailored in the light of the following requirements: (i) the calciner operates at higher temperature than the carbonator, and limestone calcination is endothermal; (ii) the stream of regenerated sorbent must act as heat carrier, so to sustain the conditions in the gasifier-carbonator, since gasification reactions are overall endothermal. The flue gas leaving the combustor will be CO_2-rich, but only additional techniques (f.i., operating the reactor in oxyfuel mode, or postprocessing the flue gas, e.g., by CaL) would enable the recovery of CO_2 at concentration levels compatible with its geological storage or utilization.

The design of sorbent looping processes in DIFB reactors must take into account the following aspects: (i) sorbent deactivation (i.e., decay of CO_2 capture performance) over repeated cycling, consequence of thermal and chemical sintering and, particularly in SEG, of possible "poisoning" by sulfur-containing species, tar, and solid fuel; (ii) loss of sorbent material due to elutriation, that may be enhanced by attrition and fragmentation.[14–17] Occurrence of (i) and (ii) requires continuous make-up of fresh sorbent to compensate for losses of sorbent uptake performance: "chemical" loss due to sintering, "physical" loss due to elutriation.

The application of the CaL concept to carry out SEG is therefore a potential way to increase the gasification efficiency. Despite similarities between CaL and the SEG process depicted in Figure 1, it is important to highlight that the typical operating conditions of CaL, which essentially is a postcombustion CO_2 capture and concentration process, are different from those of interest in this context, for example, in terms of composition of gaseous atmospheres and operating temperatures for both calcination and carbonation stages. Literature reports details on gasifier performance, reactor design, and process analysis when a Ca-based sorbent is used as a mean to push the syngas composition toward higher purity in H_2.[18–25] SEG is generally ascribed to the class of sorption-enhanced reforming processes, with literature investigating the integration with a Ca-based sorbent.[26–28] Specific aspects about sorbent behavior are present in these articles, but there are issues still deserving investigation,[7,25] as the focus on the effect that the operating conditions typical for a SEG process based on CaL concept have on sorbent CO_2 capture ability and attrition tendency, which is different from what retrieved in pure CaL studies by virtue of the differences commented above.

In this framework, our contribution in this research article is focused on the sorbent CO_2 uptake performance and attrition/fragmentation tendency when operating conditions simulating those of a DIFB-SEG process are adopted. To this end, experiments were carried out on a commercial Italian limestone in a laboratory-scale DIFB reactor, by voluntarily excluding the effect of the solid fuel. In particular, the influence of temperature and the effect of steam in the carbonator were specifically scrutinized. Quantitative data referring to carbonation degree and elutriation rate are discussed, the first aspect being crucial for the process efficiency, and the second one relevant when the large fine particle loadings often reported at the cyclones of pilot scale units are considered. Moreover, a topic very rarely addressed in the pertinent literature is the impact fragmentation tendency of sorbent particles under DIFB-SEG conditions: this is a phenomenon related to the impact of particles against targets (reactor walls, other bed particles) according to the complex fluid-dynamics of FB systems, where the formation of fragments determines the shift of the sorbent particle size distribution (PSD) toward finer sizes with consequences on both solid residence time distribution and particle reactivity toward CO_2. This article reports on this issue as well, through *ex situ* experiments carried out in an impact test rig on DIFB-SEG preprocessed sorbent samples.

2 | DESCRIPTION OF THE EXPERIMENTAL CAMPAIGN

The experimental campaign was conducted in a laboratory-scale twin interconnected FB reactor, purposely designed for looping tests. The "Twin Bed" apparatus (Figure 2) consists of two identical bubbling fluidized beds operated as calciner and carbonator, respectively. The two reactors are electrically heated and have inner diameter of 40 mm. They are divided in three sections: a wind box (0.66 m height) acting

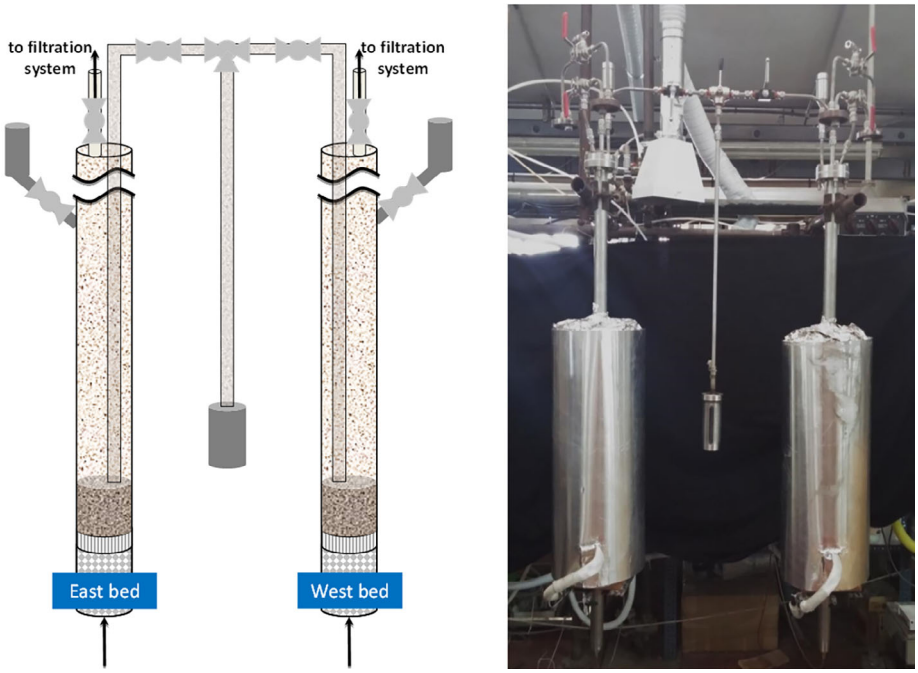

FIGURE 2 The "Twin Bed" reactor used for simulated DIFB-SEG tests (left: scheme; right: picture). DIFB, dual interconnected fluidized beds; SEG, sorption-enhanced gasification

also as gas preheater; the fluidized bed (1.0 m height), separated from the wind box by a perforated plate; the exit section, with an exhaust duct whence the flue gas is conveyed, via a valves system, to sintered steel filters (efficiency >99% for >10 μm particles) for collection of elutriated fines. A steel hopper for solid feeding is connected sideways to each reactor. Both reactors are independently operated in batch mode with respect to the solids. They are connected to each other by a duct (inner diameter of 10 mm), partially immersed in the beds, used for fast pneumatic conveying of the sorbent between the two reactors. The transfer of sorbent is accomplished by opening the valve located on the duct while acting on the valves located at the reactors' exhaust to generate the required pressure drop between the two reactors. The key advantage of this experimental setup is that it enables to reproduce a realistic particle thermal, chemical, and mechanical history, while preserving simplicity and manageability of the experimental protocol and reactor operation. A complete description of the apparatus is reported by Coppola et al.[29]

The sorbent used in the investigation was an Italian limestone ("Massicci," almost pure $CaCO_3$). Cylinders of CO_2 and N_2, and a steam generation system (Bronkhorst CEM - Controlled Evaporator and Mixer), equipped with a flow meter/controller, were used to produce surrogate flue gases to simulate SEG conditions. A "test" consisted of 10 complete cycles of calcination/carbonation, plus an 11th calcination stage (resulting in 21 total stages). The initial charge of limestone was $m_0 = 10$ g, sieved in the size range 0.4–0.6 mm. At the beginning of the test, the sorbent was fed to the calciner. Silica sand (size 0.85–1 mm) was used in both reactors as fluidization/thermal ballast material, to limit both temperature fluctuations due to chemical reactions and reactor temperature variations as the sorbent is conveyed from one reactor to the other. Sand proved to be chemically inert and with negligible contribution to attrition/fragmentation of the sorbent. For all the tests (Table 1), calcination was performed at $T = 850°C$ fluidizing the bed with a stream of 10% (by volume) CO_2 (balance air) to simulate oxidizing conditions typical of the combustor-calciner (Figure 1). In the carbonation stage, the temperature was varied in the range 600–700°C and the CO_2 concentration was set at 10% by volume. Carbonation was carried out either in absence or in presence of steam (when present, steam was 10% by volume). The balance was always N_2 in this stage, with an effort to simulate, although partly, reducing conditions typical of the gasifier-carbonator (Figure 1 where, actually, other reducing gases would be present, like as H_2 and CO). Experiments were performed under six different carbonation operation conditions, with variable temperature and steam concentration (Table 1). Each calcination or carbonation stage lasted for 10 min, a time long enough to observe practical completion of the reactions. Both the beds were fluidized at a superficial velocity of 0.5 m/s, at process conditions, that is, twice the minimum fluidization velocity. This value optimizes the segregation between sorbent and bed material (silica sand), which is crucial to have a good pneumatic transport of the sorbent between the two reactors, and to minimize sand transport.[29] The apparatus at hand results under fluidized bed bubbling conditions, which is typical for FB gasifiers.

During each carbonation stage, the CO_2 concentration at the exhaust was continuously monitored by a NDIR analyzer and the uptake of CO_2 was calculated by working out the time series of CO_2 exit concentration. The CO_2 specific capture performance ξ was calculated as the mass of CO_2 captured in a stage per mass of initial sorbent, according to

$$\xi = \frac{\int_0^t \left[W_{CO_2}^{in} - W_{CO_2}^{out}(t) \right] dt}{m_0}, \quad (1)$$

TABLE 1 Operating conditions of simulated DIFB-SEG tests

	Calcination	Carbonation					
		T600D	T600W	T650D	T650W	T700D	T700W
Temperature (°C)	850	600	600	650	650	700	700
CO_2 (% v.)	10	10	10	10	10	10	10
Air (% v.)	90	–	–	–	–	–	–
H_2O (% v.)	–	–	10	–	10	–	10
N_2 (% v.)	–	90	80	90	80	90	80

Note: The carbonation conditions have been labeled T_{ab}, where a is the temperature (600°C, 650°C, 700°C) and b is "D" for "dry" conditions and "W" for "wet" conditions.
Abbreviations: DIFB, dual interconnected fluidized beds; SEG, sorption-enhanced gasification.

where W is mass flow rates and t is the time. It is, thus, highlighted that the reference mass of sorbent in Equation (1) is $m_0 = 10$ g (the initial charge of limestone, and not the mass of active CaO stage by stage), in accordance with the definition of ξ given in our previous studies. Data of ξ were equivalently expressed in terms of X_{Ca}, the carbonation degree of Ca, that is, the moles of Ca reacted to $CaCO_3$ with respect to the moles of Ca initially charged in the DIFB system, where MW is the molecular weight:

$$X_{Ca} = \frac{MW_{CaCO_3}}{MW_{CO_2}}\xi. \quad (2)$$

The sorbent attrition rate was determined by working out the mass of fines elutriated at the exhaust and collected in the filters. The specific elutriation rate E is defined as the mass of sorbent fines cumulatively collected over a stage (calcination or carbonation), m_{el}, divided by the initial mass of sorbent and by the duration of the stage itself, Δt:

$$E = \frac{m_{el}}{m_0 \cdot \Delta t}. \quad (3)$$

When sorbent particles are processed in full-scale fluidized bed environment, they also undergo fragmentation by impact damage, related to high-velocity collisions between fluidized particles and targets (bed internals or other bed solids).[16,30–32] These collisions can be experienced by the particles in the jetting region of the FB reactor, as well as in the exit region of the riser and the cyclone, or in reactor constrictions, if present. Depending on the extent and pattern of impact fragmentation, coarse (nonelutriable) and fine (elutriable) fragments can be generated. In this study, scale and fluid-dynamics of the laboratory DIFB system would not promote impact fragmentation conditions; therefore, the phenomenon was specifically addressed in an *ex situ* apparatus reported in Figure 3, based on the concept of entraining particles in a gas stream at controlled velocity and impacting them against a target. The system consists of a vertical stainless steel eductor tube (ET), 1 m high, inner diameter 10 mm, equipped with a particle feeder (a stainless steel hopper). A controlled air flow enters the top section of the ET. The sorbent particles contained in the hopper are transported through the tube, accelerated by the air flow. When the particles exit the ET, they impact on a rigid target plate placed in a glass collection chamber 50 mm below the bottom end of the tube. The target is made of stainless steel and is inclined by 30° with respect to the horizontal. The particle impact velocity v is calculated as the sum of the gas velocity in the ET and the particle terminal velocity. This means that particle acceleration to this velocity is

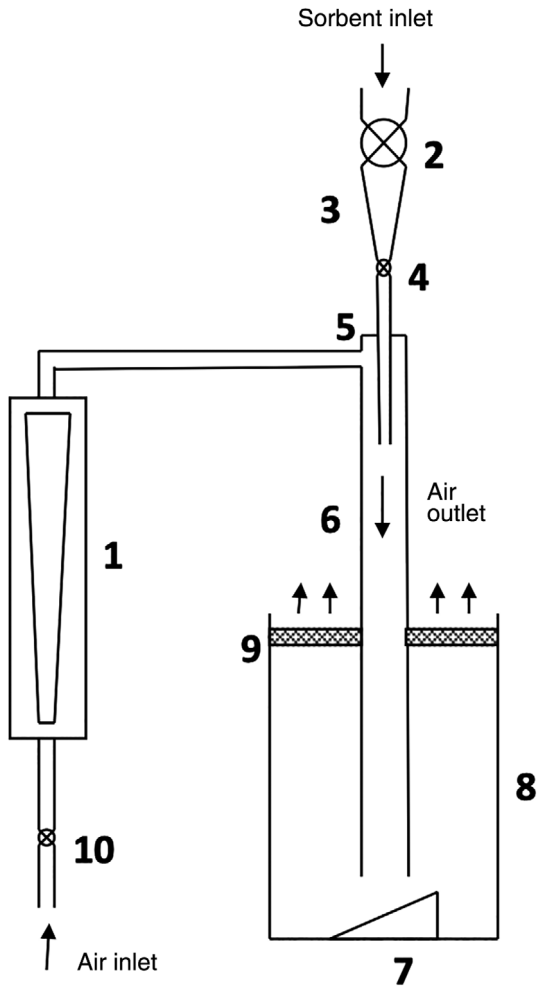

FIGURE 3 Scheme of the *ex situ* impact testing apparatus (1: gas flowmeter; 2 and 4: lock hopper valves; 3: hopper; 5: feeding tube; 6: eductor tube; 7: target plate; 8: collection chamber; 9: cellulose filter; 10: gas flow metering valve)

complete before impact as confirmed by calculations and by particle tracking at the exit of the ET with a high-speed (10,000 frames per second) video camera (Photron Ultima APX).[31] After impact, the debris can be retrieved from the collection chamber, for PSD analysis. Full description of the system can be found in Coppola et al.[16] This apparatus was conceived by the authors basing on literature works.[33–37] It is different from the standard ASTM (D5757-11) jet-cup apparatus, typically used for abrasion testing of granular materials. The present device specifically serves to study particle attrition under high-velocity impacts, but without the parallel presence of surface abrasion (unavoidable, instead, in the ASTM apparatus). In this way, the two different contributions to attrition (abrasion vs. impact fragmentation) could be independently measured without mutual interference.

Preprocessed samples (1.0 g) subjected to *ex situ* impact fragmentation tests were those arising from DIFB tests carried out under the six different operating conditions (Table 1), at the end of the 11th calcination stage, separated from sand by a 0.71 mm-sieve and resieved in the reference particle size range 0.4–0.6 mm. Impact tests were conducted at room temperature with values of v ranging from 17 to 45 m/s (each of the six DIFB samples was tested for five different impact velocities). These velocities were selected to reproduce realistic impact conditions that are likely to establish in FB systems. The cumulative PSD of impacted fragments was obtained by mechanical sieving. Finally, defining $x(d_i)$ the mass fraction of particles falling in a size interval with mean diameter d_i, we consider as "fragments" the impacted particles finer than 0.4 mm (the lower limit of the particle size range of the inlet sample), and therefore the cumulative mass fraction of fragments f reads

$$f = \sum_{d_i < 0.4\,\mathrm{mm}} [x(d_i)], \tag{4}$$

Values of f can be obtained as a function of v for each sample. Data of f vs. v were plotted on a log–log chart, to better highlight the establishment of power-law relationships, $f \propto v^k$, between mass fraction of fragments and impact velocity.

3 | RESULTS AND DISCUSSION

3.1 | CO_2 capture performance of the sorbent in DIFB-SEG tests

Figure 4 reports the values of ξ (Equation (1)) along with the number N of carbonation stages for all the simulated DIFB-SEG tests (Table 1). The effect of thermal sintering is evident from the decline of ξ on iterated calcination/carbonation cycles. The decay is very pronounced after the first cycles, to slow down thereafter. We will use T600D as the reference base-case, for which $\xi(N = 1) = 0.199$ g/g, corresponding to a carbonation conversion degree $X_{Ca} = 45.2\%$, and $\xi(N = 10) = 0.030$ g/g ($X_{Ca} = 6.8\%$). The effect of temperature may be appreciated by comparing the reference case with T650D (where

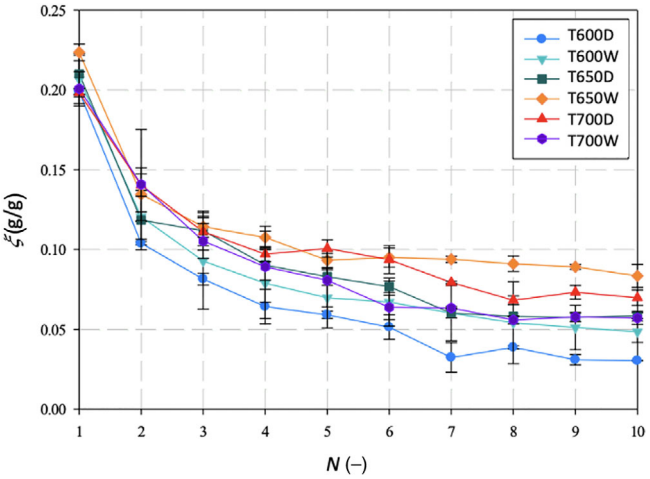

FIGURE 4 Specific CO_2 capture performance ξ as a function of the number N of carbonation stage for DIFB-SEG tests. Operating conditions listed in Table 1. Each experiment was repeated three times and bars representing minimum and maximum values are reported together with the average measure. DIFB, dual interconnected fluidized beds; SEG, sorption-enhanced gasification

X_{Ca} decreases from 47.7% [$N = 1$] to 13.4% [$N = 10$]) and T700D (where X_{Ca} decreases from 45.0% [$N = 1$] to 15.9% [$N = 10$]): the value of the carbonation degree averaged over 10 carbonation stages increases from 15.7% to 23.4% when the temperature increases from 600°C to 700°C in absence of steam (Figure 5): a positive effect of T is suggested, due to the enhanced chemical kinetics and CO_2 solid diffusion. A further proof of this behavior can be found in Figure 6, where the measured trends of outlet CO_2 concentration vs. time are reported for tests carried out under dry conditions at the three temperatures (reference carbonation stage $N = 1$). The carbonation process can be subdivided in two phases: a first one (phase "A") controlled by chemical kinetics, and a second one (phase "B") ruled by CO_2 diffusion in sorbent pores and through the carbonate layer.[38] The kinetic stage is mostly represented by the fast decrease in outlet CO_2 concentration (fast capture of CO_2 by CaO sorbent). The diffusive stage is mainly characterized by the subsequent slow increase in the curve, which is actually slower (i.e., better CO_2 capture) when T increases. Of course, even higher carbonation temperatures, not considered in this study, would sooner or later bring about thermodynamic limitations, and hamper the course of exothermal carbonation.

Also in presence of steam (Figures 4 and 5), the comparison of tests at 600°C vs. 650°C confirms that increasing T exerts a positive effect: for T600W, it is $X_{Ca} = 47.0\%$ for $N = 1$ and $X_{Ca} = 10.9\%$ for $N = 10$ (average 19.4%), while for T650W, it is $X_{Ca} = 50.8\%$ for $N = 1$ and $X_{Ca} = 19.1\%$ for $N = 10$ (average 25.6%). Moreover, the presence of steam during the carbonation stage exerts a positive influence on the overall performance of the sorbent, as inferred by comparing, respectively, the results for T600W vs. T600D, and T650W vs. T650D. This positive effect can be associated with the enhanced diffusion of CO_2 inside the porous network of the sorbent particle in presence of steam, with the development of a more favorable sorbent morphology and energy related to the CO_2 capture process by CaO,

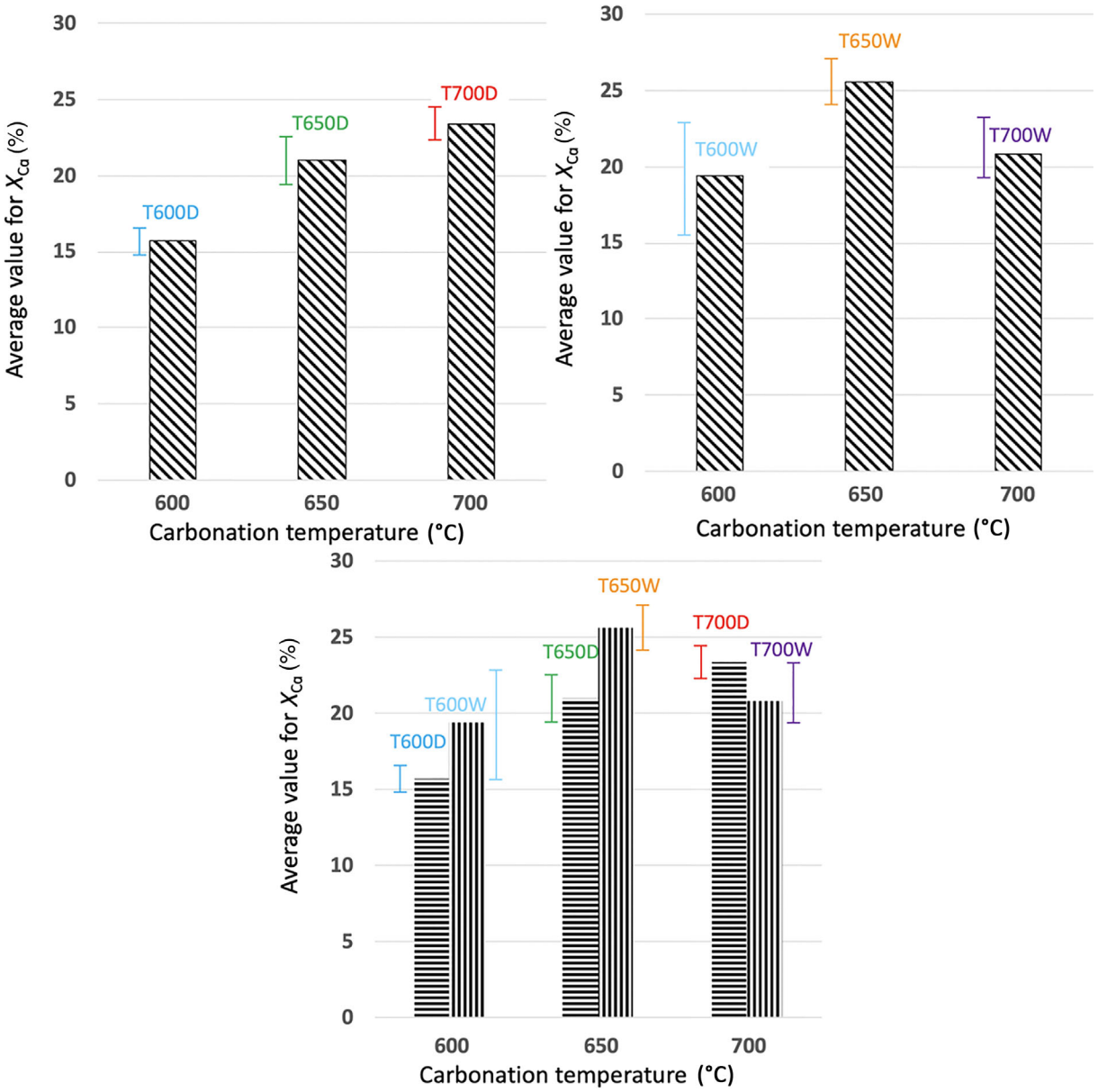

FIGURE 5 Effect of carbonation conditions on the carbonation degree averaged over 10 stages: role of temperature in absence (up-left) and presence (up-right) of steam, and role of steam (down). Bars represent minimum and maximum values for the average carbonation degree (three repetitions)

along with the formation of ionic (OH^-) species, in presence of H_2O, as widely discussed in literature.[3,15,39–45] On the other hand, at higher temperature, H_2O starts to promote sorbent sintering phenomena,[46,47] and this could explain why T700W ($N = 1 \rightarrow X_{Ca} = 45.4\%$ and $N = 10 \rightarrow X_{Ca} = 12.9\%$; average 20.8%) did not show the best result among the tests.

The highest and lowest values of ξ were obtained under T650W and T600D reaction conditions, respectively. If we compare these data with those obtained under conventional CaL conditions,[44] it may be stated that the more severe CaL calcination temperature (>900°C), required by thermodynamics constraints due to the CO_2 richer calciner atmosphere, brings about more extensive sintering resulting in far less efficient CO_2 capture, an aspect also discussed by Tregambi et al.[48]

The absence of fuel in the simulated tests can of course influence the sorbent performance, due to the contextual absence of other gases (e.g., H_2, CH_4, CO, NO_x) that could have an effect on CO_2 capture. This will be verified in the future with devoted tests. Anyway, from the profiles of CO_2 capture decay (cf. Figure 4) it is possible to extrapolate data useful for the correct design of the system.[49]

3.2 | In-bed sorbent attrition

The specific elutriation rate E (Equation 3) was determined from the amount of sorbent collected at the exhaust during calcination and carbonation stages. Table 2 reports its average value (over the 21 stages of each test), in the range 0.017–0.038 $\times$ 10^{-3} min^{-1}, corresponding

to an average fractional loss of sorbent per stage in the range 0.017%–0.038% with respect to the initial mass of sorbent (each stage lasts 10 min). An interesting correlation may be generally established between the extent of CO_2 uptake and sorbent elutriation tendency by attrition. Operating conditions that give rise to enhanced CO_2 capture yield sorbent samples characterized by larger fractional content of $CaCO_3$. It is here assumed that the latter, harder than CaO, can concentrate near the outer surface of the particle, according to a core-shell pattern as discussed in literature,[10,38,50] exposed to attrition by surface wear under fluidized conditions. This argument supports the finding that larger values of ξ are typically associated with lower values for E (Figure 7). Actually, the case with the lowest elutriation rate, T650W, is the one with the highest average carbonation degree—vice versa for the T600D sample. It is highlighted here that the correlation suggested in Figure 7 was not strictly observed among all the six investigated cases: for example, the T700D case shows a slightly higher average value for CO_2 capture performance than T650D (Figure 5), and a slightly larger mean value for specific elutriation rate (Table 2) as well. Minor effects related to operating temperature (able to fragilize the particle structure) might be at work in this case. Finally, reported data can be useful to extrapolate possible attrition data at large scale by means of established equations in literature reporting E vs. operating conditions.[51]

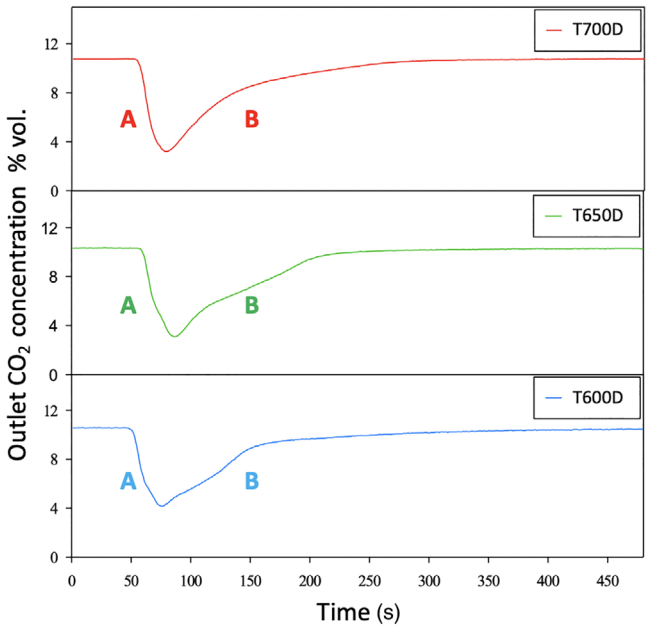

FIGURE 6 Trends of outlet CO_2 concentration vs. time for T600D (down), T650D (middle), and T700D (up) conditions during the first ($N = 1$) carbonation stage ("A" = kinetics-controlled stage; "B" = solid diffusion-controlled stage)

3.3 | Impact fragmentation for sorbent preprocessed in DIFB-SEG tests

Cumulative PSD and log–log f vs. v plot are reported in Figures 8 and 9, respectively, for debris analyzed after impact tests on the preprocessed DIFB-SEG samples. We start our analysis with the T600D case (meaning that the impact tests have been carried out on samples preprocessed in the DIFB system under the T600D operating conditions reported in Table 1). As expected, the fragments size distribution is progressively shifted toward finer sizes as v increases (Figure 8) and the cumulative mass fraction of fragments increases with the impact velocity as a consequence of the higher energy associated with the impact event (Figure 9): f is around 1%–3% up to a critical velocity* $v^* = 31$ m/s, then a marked slope change in the $f(v)$ curve is observed with f increasing up to 13% at $v = 45$ m/s, suggesting that k, the exponent of the power-law $f(v)$ relationship, increases when v trespasses v^* (it is $k = 1.21$ for $v \le v^*$, $k = 3.89$ for $v \ge v^*$; for a better visibility, data for T600D are separately illustrated in Figure 10) so underlining the more relevant mass production of fragments at higher velocities of impact. For low impact velocities (i.e., low impact energy, $v \le v^*$), the propagation of fractures due to the impact event is mostly confined at the particles' surface, so mostly producing fine chips (that can be seen as fragments of size much finer than the parent particle size). When the energy associated to the impact event increases, the fractures can propagate throughout the particle giving rise to the splitting of the parent particles into fragments of comparable size (see Figure 10; for a deeper analysis of chipping and splitting phenomena, the reader is referred to our previous studies[16,31]). Consequently, splitting ends up into a more relevant mass production of fragments, as seen from the values of k in chipping and splitting regimes (Figure 10). This chipping/splitting pattern can be applied to semibrittle materials, as it might be the case for a sorbent sample preprocessed (and, then, partly thermally sintered) for many cycles during DIFB-SEG operation.

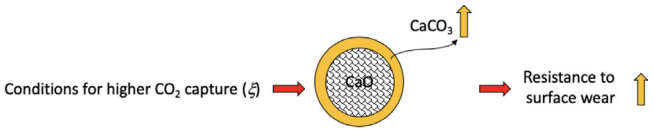

FIGURE 7 Relationship between CO_2 capture performance and resistance to attrition by surface wear

TABLE 2 Mean value (over 21 stages) of the specific elutriation rate for DIFB-SEG tests

	T600D	T600W	T650D	T650W	T700D	T700W
$\bar{E} \times 10^3$ (min^{-1})	0.038	0.028	0.030	0.017	0.032	0.022
σ (min^{-1})	0.0016	0.0011	0.0029	0.0008	0.0050	0.0011

Note: Values averaged over three repeated tests and reported along with standard deviation σ, calculated based on $\bar{E} \times 10^3$ values.
Abbreviations: DIFB, dual interconnected fluidized beds; SEG, sorption-enhanced gasification.

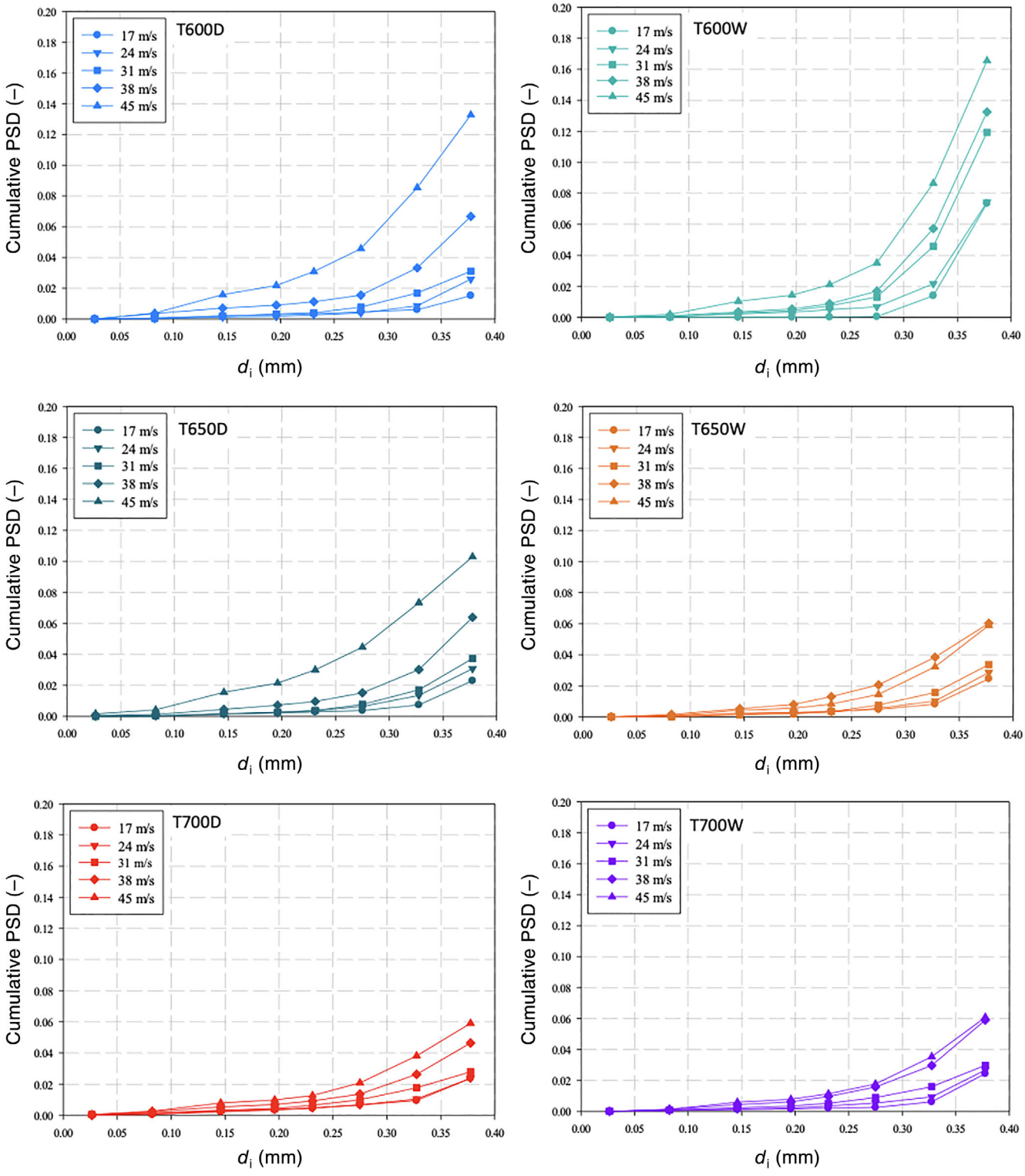

FIGURE 8 Cumulative particle size distributions of fragments (d_i < 0.4 mm) as a function of the impact velocity (reported in legend) for samples preprocessed in DIFB-SEG tests and then tested in the *ex situ* impact apparatus. DIFB, dual interconnected fluidized beds; SEG, sorption-enhanced gasification

Similar trends were also generally observed for other samples, with f in the range 2%–4% in the chipping regime, then increasing up to 6%–10% (at $v = 45$ m/s) in the splitting regime. It must be here recalled that the DIFB-SEG samples were subjected to impact tests after the 11th calcination in the fluidized bed system: as calcination is a chemical reaction substantially complete under the adopted operating conditions (850°C in 10/90 CO_2/air atmosphere for all samples), an aspect experimentally verified by the analysis of CO_2 concentration time series at the calciner exhaust, the sorbent samples can be considered as mostly constituted by CaO. Therefore, their tendency to

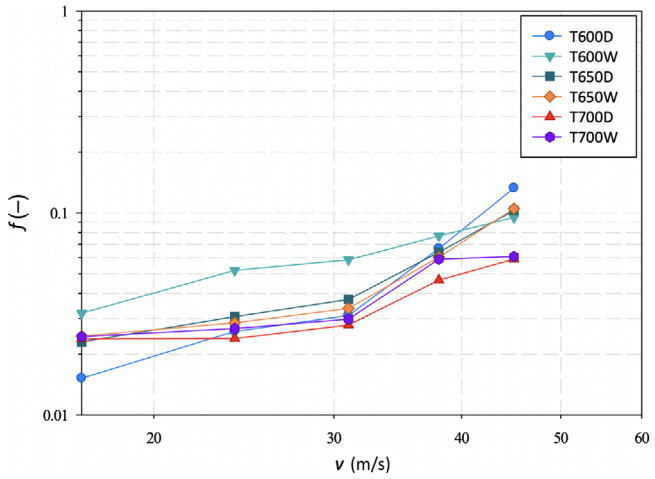

FIGURE 9 Cumulative mass fraction of fragments vs. impact velocity (log–log plot) for samples preprocessed in DIFB-SEG tests and then tested in the *ex situ* impact apparatus. DIFB, dual interconnected fluidized beds; SEG, sorption-enhanced gasification

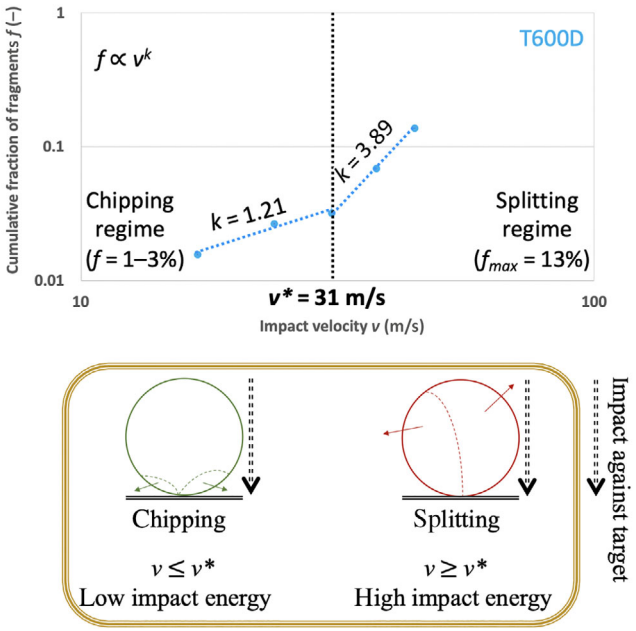

FIGURE 10 Cumulative mass fraction of fragments vs. impact velocity (log–log plot) for T600D sample (from Figure 9) with information on chipping and splitting regimes (up) and illustration of particle chipping/splitting at increasing velocity of impact against a solid target, for semibrittle materials (down)

impact fragmentation can be here ruled by physical, rather than chemical (i.e., effect of the carbonate shell) properties. As depicted in Figure 11, the average value of *f* (over the five values of *v*) generally decreases as the carbonation temperature, to which the sorbent was subjected in the DIFB process, increases in the carbonation temperature range 600–700°C. This can be related to enhanced hardening (→more resistant particle) promoted by the process temperature. On the other hand, in the *T* range investigated, no clear effect of the presence of water vapor (vs. its absence) was observed. It is here

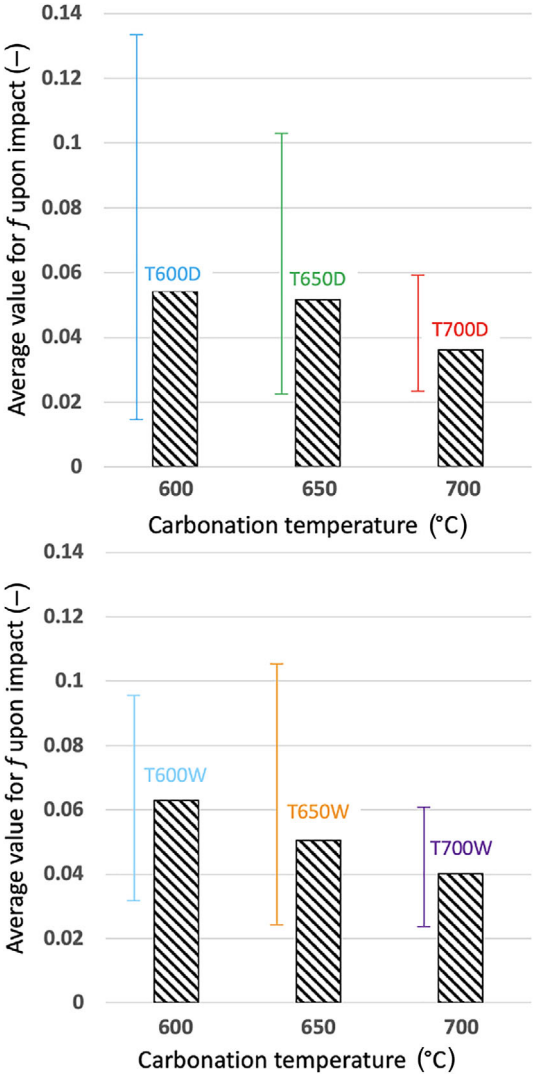

FIGURE 11 Average value for *f*, the cumulative mass fraction of fragments collected upon impact at different velocities, as a function of the DIFB preprocessing carbonation temperature: absence of vapor (up), presence of vapor (down). Bars represent minimum and maximum values (for each case) of the range that generates the average *f* value. DIFB, dual interconnected fluidized beds

underlined that, in a real system, sorbent particles would be subjected to a field of impact velocities whose characteristics depend on the actual hydrodynamics of the system. In this sense, the average value of *f* can represent a first indicator of the particles tendency to undergo impact fragmentation.

4 | CONCLUSIONS

When processed at carbonation temperature increasing from 600°C to 700°C in a DIFB system under operating conditions simulating those of SEG, sorbent samples of the investigated limestone were characterized by higher performance of CO_2 uptake due to enhanced kinetics and CO_2 diffusion within the solid particle. In absence of water vapor, the calcium carbonation degree averaged over 10 cycles

was 15.7%, 21.0%, and 23.4% at 600°C, 650°C, and 700°C, respectively. This, in turn, led to particles with increased mechanical resistance thus generally increasing the particles resistance to surface wear phenomena (the average value of fines elutriation rate decreased, with respect to the operation at 600°C, by about 16% at 700°C). Moreover, higher carbonation temperature can increase particle hardening phenomena so making samples more resistant to impact fragmentation: the average value of the cumulative mass fraction of impacted fragments decreased, with respect to the sample preprocessed at 600°C (it is 5.43%), by about 5% and 33% when the sorbent was preprocessed at 650°C and 700°C, respectively. In presence of water vapor on carbonation, the CO_2 capture performance was even higher if a temperature of 600°C or 650°C was adopted (average carbonation degree = 19.4% and 25.6%, respectively), due to the carbonation-promoting effects (enhanced diffusion of CO_2 inside the porous network of the sorbent particle, development of a more favorable sorbent morphology and energy related to the CO_2 capture process by CaO, formation of ionic species) in the presence of steam, as reported in literature. On the other hand, at 700°C steam can exert a relevant, undesired, sintering effect that partly limits the carbon dioxide uptake by sorbent particles (average carbonation degree = 20.8%). The positive effect of preprocessing the samples at a higher temperature on their impact fragmentation tendency was observed also in presence of water vapor on carbonation: the average value of the cumulative fraction of impacted fragments decreased, with respect to the sample preprocessed at 600°C (it is 6.29%), by about 36% when the sorbent was preprocessed at 700°C. Impact fragmentation patterns of investigated samples followed a chipping/splitting paradigm as the impact velocity increased in a range reproducing realistic values that are likely to establish in fluidized bed systems.

In conclusion, taking for granted the presence of steam in the gasifier-carbonator, an optimal carbonation temperature of 650°C is suggested for this limestone in terms of both satisfying CO_2 uptake and limited tendency to attrition/fragmentation. Results here presented can be useful for the determination of the make-up of fresh sorbent required for steady operation, and for optimal design and operation of SEG. To this end, further study on this research line should concern the possible extension of operating conditions/techniques and generalization of the results to other limestones (characterized by different physicochemical features, such as porosimetric texture), the morphological characterization of sorbent samples treated under the different operating conditions, and the integration of the present outcomes into process schemes entailing concurrent solid fuel gasification/combustion and CaL in fluidized bed systems.

ACKNOWLEDGMENTS

The financial support related to the Project "Mi-BESt: Micro co/tri generazione di Bioenergia Efficiente e Stabile," funded by the Italian government, is gratefully acknowledged, as well as the experimental support of the students Mr. Mario Paolo Scolaro and Mr. Vincenzo Marotta. Open Access Funding provided by Universita degli Studi di Napoli Federico II within the CRUI-CARE Agreement.

AUTHOR CONTRIBUTIONS

Antonio Coppola: Conceptualization (equal); data curation (equal); formal analysis (equal); investigation (equal); methodology (equal); supervision (equal); validation (equal); writing – review and editing (equal). **Aida Sattari:** Investigation (equal); methodology (equal). **Fabio Montagnaro:** Conceptualization (equal); data curation (equal); formal analysis (equal); supervision (equal); validation (equal); writing – original draft (equal); writing – review & editing (equal). **Fabrizio Scala:** Conceptualization (equal); data curation (equal); formal analysis (equal); supervision (equal); validation (equal); writing – review and editing (equal). **Piero Salatino:** Conceptualization (equal); formal analysis (equal); supervision (equal); writing – review and editing (equal).

DATA AVAILABILITY STATEMENT

The data that support the findings of this study are available from the corresponding author upon reasonable request.

NOTATION

CaL	calcium looping
DIFB	dual interconnected fluidized beds
ET	eductor tube
PSD	particle size distribution
SEG	sorption-enhanced gasification
d_i	mean particle diameter (mm)
E	specific elutriation rate (1/min)
f	cumulative fractional mass of sorbent fragments obtained in impact tests (−)
k	exponent of the power-law $f(v)$ relationship (−)
m_0	initial mass of sorbent (g)
m_{el}	mass of elutriated fines over a stage (g)
MW	molecular weight
N	number of carbonation stages (−)
T	temperature (°C)
t	time (min)
v	particle impact velocity (m/s)
v^*	critical impact velocity (m/s)
W	CO_2 mass flow rate (g/min)
x	mass fraction in particle size distribution (−)
X_{Ca}	Ca carbonation degree (−)

GREEK SYMBOLS

ξ	CO_2-specific capture performance (−)
σ	standard deviation for values of E (1/min)

ORCID

Fabio Montagnaro https://orcid.org/0000-0002-6377-3989

ENDNOTE

* The critical impact velocity is evaluated by the intercept (in the mass fraction of fragments vs. particle impact velocity log–log chart) between the straight line at low velocity, typical of chipping, and that at higher velocity typical of splitting mode (see Figure 10).

REFERENCES

1. Florin NH, Harris AT. Enhanced hydrogen production from biomass with in situ carbon dioxide capture using calcium oxide sorbents. *Chem Eng Sci*. 2008;63:287-316.
2. Sutton D, Kelleher B, Ross JRH. Review of literature on catalysts for biomass gasification. *Fuel Process Technol*. 2001;73:155-173.
3. Fuchs J, Schmid JC, Müller S, Hofbauer H. Dual fluidized bed gasification of biomass with selective carbon dioxide removal and limestone as bed material: a review. *Renew Sust Energy Rev*. 2019;107:212-231.
4. Blamey J, Anthony EJ, Wang J, Fennell PS. The calcium looping cycle for large-scale CO_2 capture. *Prog Energy Combust Sci*. 2010;36:260-279.
5. Rodríguez N, Alonso M, Abanades JC. Experimental investigation of a circulating fluidized-bed reactor to capture CO_2 with CaO. *AIChE J*. 2011;57:1356-1366.
6. Erans M, Manovic V, Anthony EJ. Calcium looping sorbents for CO_2 capture. *Appl Energy*. 2016;180:722-742.
7. Perejón A, Romeo LM, Lara Y, Lisbona P, Martínez A, Valverde JM. The calcium-looping technology for CO_2 capture: on the important roles of energy integration and sorbent behaviour. *Appl Energy*. 2016;162:787-807.
8. Salaudeen SA, Acharya B, Dutta A. CaO-based CO_2 sorbents: a review on screening enhancement, cyclic stability, regeneration and kinetics modelling. *J CO2 Util*. 2018;23:179-199.
9. Coppola A, Senneca O, Scala F, Montagnaro F, Salatino P. Looping cycles for low carbon technologies: a survey of recent research activities in Naples. *Fuel*. 2020;268:117371.
10. Chen J, Duan L, Sun Z. Review on the development of sorbents for calcium looping. *Energy Fuel*. 2020;34:7806-7836.
11. Di Lauro F, Tregambi C, Montagnaro F, Salatino P, Chirone R, Solimene R. Improving the performance of calcium looping for solar thermochemical energy storage and CO_2 capture. *Fuel*. 2021;298:120791.
12. Göransson K, Söderlind U, He J, Zhang W. Review of syngas production via biomass DFBGs. *Renew Sust Energy Rev*. 2011;15:482-492.
13. Kirnbauer F, Hofbauer H. Investigation on bed material changes in a dual fluidized bed steam gasification plant in Güssing, Austria. *Energy Fuels*. 2011;25:3793-3798.
14. Alonso M, Arias B, Fernández JR, Bughin O, Abanades C. Measuring attrition properties of calcium looping materials in a 30 kW pilot plant. *Powder Technol*. 2018;336:273-281.
15. Coppola A, Esposito A, Montagnaro F, Iuliano M, Scala F, Salatino P. The combined effect of H_2O and SO_2 on CO_2 uptake and sorbent attrition during fluidised bed calcium looping. *Proc Combust Inst*. 2019;37:4379-4387.
16. Coppola A, Montagnaro F, Scala F, Salatino P. Impact fragmentation of limestone-based sorbents for calcium looping: the effect of steam and sulphur dioxide. *Fuel Process Technol*. 2020;208:106499.
17. Miao M, Deng B, Yao X, Wei G, Zhang M, Yang H. Experimental study on calcination and fragmentation characteristics of limestone in fluidized bed. *J Energy Inst*. 2021;95:206-218.
18. Han L, Wang Q, Yang Y, Yu C, Fang M, Luo Z. Hydrogen production via CaO sorption enhanced anaerobic gasification of sawdust in a bubbling fluidized bed. *Int J Hydrogen Energy*. 2011;36:4820-4829.
19. Gazzani M, Macchi E, Manzolini G. CO_2 capture in integrated gasification combined cycle with SEWGS – part a: thermodynamic performances. *Fuel*. 2013;105:206-219.
20. Kuo PC, Chen JR, Wu W, Chang JS. Integration of calcium looping technology in combined cycle power plants using co-gasification of torrefied biomass and coal blends. *Energ Conver Manage*. 2018;174:489-503.
21. Chen S, Zhao Z, Soomro A, et al. Hydrogen-rich syngas production via sorption-enhanced steam gasification of sewage sludge. *Biomass Bioenergy*. 2020;138:105607.
22. Martínez I, Kulakova V, Grasa G, Murillo R. Experimental investigation on sorption enhanced gasification (SEG) of biomass in a fluidized bed reactor for producing a tailored syngas. *Fuel*. 2020;259:116252.
23. Pitkäoja A, Ritvanen J, Hafner S, Hyppänen T, Scheffknecht G. Simulation of a sorbent enhanced gasification pilot reactor and validation of reactor model. *Energ Conver Manage*. 2020;204:112318.
24. Mbeugang CFM, Li B, Lin D, et al. Hydrogen rich syngas production from sorption enhanced gasification of cellulose in the presence of calcium oxide. *Energy*. 2021;228:120659.
25. Parvez AM, Hafner S, Hornberger M, Schmid M, Scheffknecht G. Sorption enhanced gasification (SEG) of biomass for tailored syngas production with in-situ CO_2 capture: current status, process scale-up experiences and outlook. *Renew Sust Energy Rev*. 2021;141:110756.
26. Meyer J, Mastin J, Sanz PC. Sustainable hydrogen production from biogas using sorption-enhanced reforming. *Energy Procedia*. 2014;63:6800-6814.
27. García-Lario AL, Grasa GS, Murillo R. Performance of a combined CaO-based sorbent and catalyst on H_2 production, via sorption enhanced methane steam reforming. *Chem Eng J*. 2015;264:697-705.
28. Di Giuliano A, Gallucci K, Foscolo PU. Determination of kinetic and diffusion parameters needed to predict the behaviour of CaO-based CO_2 sorbent and sorbent-catalyst materials. *Ind Eng Chem Res*. 2020;59:6840-6854.
29. Coppola A, Scala F, Gargiulo L, Salatino P. A twin-bed test reactor for characterization of calcium looping sorbents. *Powder Technol*. 2017;316:585-591.
30. Ghadiri M, Zhang Z. Impact attrition of particulate solids. Part 1: a theoretical model of chipping. *Chem Eng Sci*. 2002;57:3659-3669.
31. Scala F, Montagnaro F, Salatino P. Attrition of limestone by impact loading in fluidized beds. *Energy Fuel*. 2007;21:2566-2572.
32. Xiao G, Grace JR, Lim CJ. Evolution of limestone particle size distribution in an air-jet attrition apparatus. *Ind Eng Chem Res*. 2014;53:15845-15851.
33. Yuregir KR, Ghadiri M, Clift R. Observations on impact attrition of granular solids. *Powder Technol*. 1986;49:53-57.
34. Scala F, Salatino P, Boerefijn R, Ghadiri M. Attrition of sorbents during fluidized bed calcination and sulphation. *Powder Technol*. 2000;107:153-167.
35. Salman AD, Biggs CA, Fu J, Angyal I, Szabó M, Hounslow MJ. An experimental investigation of particle fragmentation using single particle impact studies. *Powder Technol*. 2002;128:36-46.
36. Samimi A, Moreno R, Ghadiri M. Analysis of impact damage of agglomerates: effect of impact angle. *Powder Technol*. 2004;143–144:97-109.
37. Chen Z, Lim CJ, Grace JR. Study of limestone particle impact attrition. *Chem Eng Sci*. 2007;62:867-877.
38. Li Z, Fang F, Tang X, Cai N. Effect of temperature on the carbonation reaction of CaO with CO_2. *Energy Fuel*. 2012;26:2473-2482.
39. Donat F, Florin NH, Anthony EJ, Fennell PS. Influence of high-temperature steam on the reactivity of CaO-based sorbent in cyclic carbonation/calcination for CO_2 capture. *Environ Sci Technol*. 2012;46:1262-1269.
40. Li Z, Liu Y, Cai N. Understanding the enhancement effect of high-temperature steam on the carbonation reaction of CaO with CO_2. *Fuel*. 2014;127:88-93.
41. Zhang L, Zhang B, Yang Z, Guo M. The role of water on the performance of calcium oxide-based sorbents for carbon dioxide capture: a review. *Energ Technol*. 2015;3:10-19.
42. Yang P, Duan L, Tang H, Cai T, Sun Z. Explaining steam-enhanced carbonation of CaO based on first principles. *Greenh Gases Sci Technol*. 2018;8:1110-1123.
43. Yang P, Sun Z, Duan L, Tang H. Mechanism of steam-declined sulfation and steam-enhanced carbonation by DFT calculations. *Greenh Gases Sci Technol*. 2020;10:472-483.

44. Coppola A, Esposito A, Montagnaro F, De Tommaso G, Scala F, Salatino P. Effect of exposure to SO_2 and H_2O during the carbonation stage of fluidised bed calcium looping on the performance of sorbents of different nature. *Chem Eng J*. 2019;377:120626.
45. Wang H, Li Z, Cai N. Multiscale model for steam enhancement effect on the carbonation of CaO particle. *Chem Eng J*. 2020;394:124892.
46. Borgwardt RH. Calcium oxide sintering in atmospheres containing water and carbon dioxide. *Ind Eng Chem Res*. 1989;28:493-500.
47. Agnew J, Hampartsoumian E, Jones JM, Nimmo W. The simultaneous calcination and sintering of calcium based sorbents under a combustion atmosphere. *Fuel*. 2000;79:1515-1523.
48. Tregambi C, Di Lauro F, Montagnaro F, Salatino P, Solimene R. Calcium looping coupled with concentrated solar power for carbon capture and thermochemical energy storage. *Ind Eng Chem Res*. 2019;58:21262-21272.
49. Grasa GS, Abanades JC, Alonso M, González B. Reactivity of highly cycled particles of CaO in a carbonation/calcination loop. *Chem Eng J*. 2008;137:561-567.
50. Grasa G, Abanades JC, Anthony EJ. Effect of partial carbonation on the cyclic CaO carbonation reaction. *Ind Eng Chem Res*. 2009;48:9090-9096.
51. Scala F, Salatino P. Limestone fragmentation and attrition during fluidized bed oxyfiring. *Fuel*. 2010;89:827-832.

How to cite this article: Coppola A, Sattari A, Montagnaro F, Scala F, Salatino P. Performance of limestone-based sorbent for sorption-enhanced gasification in dual interconnected fluidized bed reactors. *AIChE J*. 2022;e17588. doi:10.1002/aic.17588